Acta Pharmaceutica Sinica B 2017;7(6):657–664

Chinese Pharmaceutical Association
Institute of Materia Medica, Chinese Academy of Medical Sciences

Acta Pharmaceutica Sinica B

www.elsevier.com/locate/apsb
www.sciencedirect.com

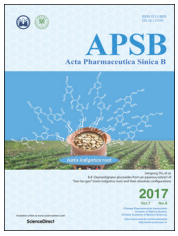

SHORT COMMUNICATION

Comparison of the inhibition potentials of icotinib and erlotinib against human UDP-glucuronosyltransferase 1A1

Xuewei Cheng[a,c,†], Xia Lv[b,c,†], Hengyan Qu[a], Dandan Li[a], Mengmeng Hu[a], Wenzhi Guo[d], Guangbo Ge[c,e,*], Ruihua Dong[a,*]

[a]*Clinical Pharmacology Laboratory, Military Academy of Medical Science Hospital, Beijing 100071, China*
[b]*College of Life Science, Dalian Nationalities University, Dalian 116600, China*
[c]*Dalian Institute of Chemical Physics, Chinese Academy of Sciences, Dalian 116023, China*
[d]*Department of Hepatobiliary and Pancreatic Surgery, The First Affiliated Hospital of Zhengzhou University, Zhengzhou 450001, China*
[e]*Institute of Interdisciplinary Medicine, Shanghai University of Traditional Medicine, Shanghai 201203, China*

Received 5 April 2017; received in revised form 15 June 2017; accepted 30 June 2017

KEY WORDS

Icotinib;
Erlotinib;
UGT1A1;
Inhibitory effects;
Drug–drug interactions (DDIs)

Abstract UDP-glucuronosyltransferase 1A1 (UGT1A1) plays a key role in detoxification of many potentially harmful compounds and drugs. UGT1A1 inhibition may bring risks of drug–drug interactions (DDIs), hyperbilirubinemia and drug-induced liver injury. This study aimed to investigate and compare the inhibitory effects of icotinib and erlotinib against UGT1A1, as well as to evaluate their potential DDI risks *via* UGT1A1 inhibition. The results demonstrated that both icotinib and erlotinib are UGT1A1 inhibitors, but the inhibitory effect of icotinib on UGT1A1 is weaker than that of erlotinib. The IC_{50} values of icotinib and erlotinib against UGT1A1-mediated NCHN-*O*-glucuronidation in human liver microsomes (HLMs) were 5.15 and 0.68 μmol/L, respectively. Inhibition kinetic analyses demonstrated that both icotinib and erlotinib were non-competitive inhibitors against UGT1A1-mediated glucuronidation of NCHN in HLMs, with the K_i values of 8.55 and 1.23 μmol/L, respectively. Furthermore, their potential DDI risks *via* UGT1A1 inhibition were quantitatively predicted by the ratio of the areas under the concentration–time curve (AUC) of NCHN. These findings are helpful for the medicinal chemists to

*Corresponding authors. Tel.: +86 411 843793171, +86 10 66947482.
E-mail addresses: geguangbo@dicp.ac.cn (Guangbo Ge), sm.8056@163.com (Ruihua Dong).
†These authors made equal contributions to this work.

Peer review under responsibility of Institute of Materia Medica, Chinese Academy of Medical Sciences and Chinese Pharmaceutical Association.

http://dx.doi.org/10.1016/j.apsb.2017.07.004

design and develop next generation tyrosine kinase inhibitors with improved safety, as well as to guide reasonable applications of icotinib and erlotinib in clinic, especially for avoiding their potential DDI risks *via* UGT1A1 inhibition.

1. Introduction

Human uridine-disphosphate glucuronosyltransferase 1A1 (UGT1A1), one of the most important phase II conjugative enzymes, is of particular importance for human health. As the sole physiologically relevant enzyme involved in the metabolic elimination of endogenous bilirubin, UGT1A1 plays key roles in preventing bilirubin accumulation to toxic levels[1]. It is well known that bilirubin, an endogenous toxic metabolite degraded from hemoglobin, can be produced appropriately 250–400 mg each day in human[2]; UGT1A1 inhibition or dysfunction may bring increased risks of bilirubin-related diseases such as hyperbilirubinemia, kernicterus and drug-induced liver injury[3]. Another biological function of UGT1A1 is the metabolism and detoxification of many xenobiotics including clinical drugs (such as etoposide and SN-38), environmental toxicants and chemical carcinogens. Inhibition of UGT1A1 may decrease the metabolic rate and increase the plasma concentration of these xenobiotics, causing severe drug–drug interactions or other undesirable effects[4]. It is noteworthy that many tyrosine kinase inhibitors (TKIs) including erlotinib, nilotinib, pazopanib, lapatinib, regorafenib and sorafenib exhibit strong inhibitory effects against UGT1A1[5–7], which is closely associated with their side effects, such as hyperbilirubinemia, liver function impairment and hepatotoxicity.

TKIs are a class of chemotherapy drugs. Such agents are commonly used for the treatment of a variety of cancers, including non-small cell lung cancer (NSCLC), head and neck, colorectal, renal, prostate, breast, and primary brain cancer[8–10]. In recent years, more than thirty TKIs have been approved for the treatment of certain forms of cancers, and several others are at various stages of clinical studies. In contrast to traditional chemotherapy drugs, most of TKIs have specific effects on target cancerous cells, and thus displayed fewer side effects and high therapeutic index in clinical. However, it has been reported that some TKIs (such as erlotinib, pazopanib, sorafenib and nilotinib) may have caused a broad set of undesirable side effects, including hyperbilirubinemia, liver injury or other safety issues[6,11]. Taking into account that UGT1A1 is the key enzyme responsible for bilirubin detoxification and that many TKIs have been proved as potent UGT1A1 inhibitors, it is necessary to investigate the inhibitory effects of newly developed TKIs on UGT1A1 and to predict the potential DDI risks of TKIs *via* UGT1A1 inhibition.

Icotinib (4-[(3-ethynylphenyl) amino]-6,7-benzo-12-crown-4-quinazoline hydrochloride Fig. 1) is a potent, oral, reversible TKI approved in 2011 by the China Food and Drug Administration (CFDA), for the treatment of advanced NSCLC patients who progressed with at least one platinum-based chemotherapy[12,13]. As a second-generation drug driving from erlotinib, icotinib has similar chemical structure and physico-chemical properties to erlotinib[13,14], while both agents act on the same target (epidermal growth factor receptor, EGFR) and display near identical clinical efficacy. Although the antitumor efficacy of icotinib has been well investigated *in vitro* and *in vivo*, icotinib-associated toxicity or side effects as well as related mechanism are rarely reported. Taking into account that UGT1A1 is a known off-target of erlotinib and other TKIs with similar structure, icotinib may target on UGT1A1 and thus evoke the safety concerns. However, the inhibitory effects and inhibition behaviors of icotinib on human UGT1A1 have not been investigated yet.

This study aimed to investigate and to compare the inhibitory effects of icotinib and erlotinib on UGT1A1. To this end, *N*-3-carboxy propyl-4-hydroxy-1,8-naphthalimide (NCHN), a newly reported specific fluorescent probe substrate for UGT1A1, was used to investigate the inhibitory potentials of icotinib and erlotinib on UGT1A1 in both recombinant enzymes and HLMs. The dose-dependent inhibition curves and the half maximal inhibitory concentration (IC_{50}) of icotinib and erlotinib against UGT1A1 were determined and compared for the first time. Furthermore, the inhibition kinetic analyses in both UGT1A1 and HLMs were also performed to characterize the inhibitory type and inhibition constant (K_i) of these two TKIs. In addition, the potential DDI risks were also quantitatively predicted by the ratio of the areas under the plasma drug concentration–time curve (AUC).

2. Materials and methods

2.1. Chemicals and reagents

Icotinib (purity > 98%) was purchased from Biochempartner Co., Ltd. (Shanghai, China). Erlotinib (purity > 99%) was purchased from Roche Co., Ltd. (Shanghai, China). NCHN was chemically synthesized and its glucuronidation product NCHN-*O*-glucuronide (NCHNG) was biosynthesized by authors as previously reported[4]. Uridine-5′-diphosphoglucuronic acid (UDPGA) was obtained from Sigma–Aldrich (St. Louis, MO, USA). UGT1A1 was obtained from BD Gentest (Woburn, MA, USA). HLMs, derived from 50 donors, were obtained from BioreclamationIVT (Baltimore, USA). The tissues were from both males ($n = 25$) and females ($n = 25$); the median age was 58 years with the age range

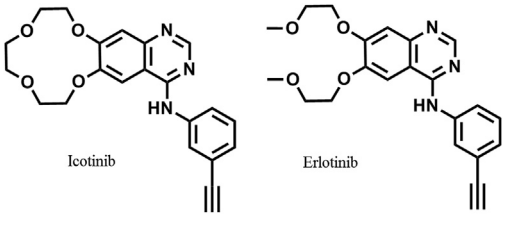

Figure 1 Chemical structures of icotinib and erlotinib.

of 17 to 89; the ethnicity were 2% Caucasian, 10% Hispanic, 4% Black, 2% Asian and 2% others. BioreclamationIVT maintained strict adherence to all applicable ethical guidelines and regulations and the tissues were directly from non-profit organization that have provided assurance as to legal compliance. BioreclamationIVT does not traffic in human tissues and has the utmost respect and appreciation for all donated tissues. Liver preparations were stored at –80 °C until use. The solvents and other reagents were of analytical reagent grade.

2.2. *Inhibition assays of NCHN-4-O-glucuronidation*

The inhibitory effects of icotinib and erlotinib against NCHN-4-*O*-glucuronidation were determined according to previously published methods with a slight modification[15]. A typical incubation mixtures (total volume 200 μL) was consisted of Tris–HCl buffer (pH 7.4, 50 mmol/L), UGT1A1 (0.06 mg/mL) or HLM (0.2 mg/mL), $MgCl_2$ (50 mmol/L), Brij 58 (0.1 mg/mg protein) and NCHN (20 μmol/L for inhibition screening; 15–100 μmol/L for inhibition constant determination) in the presence or absence of different concentrations of icotinib and erlotinib (1, 10, and 100 μmol/L for inhibition screening; 0.2–60 μmol/L for inhibition constant determination). HLMs were pre-incubated with Brij 58 on ice for 20 min before incubation. After 3 min pre-incubation at 37 °C, the reaction was initiated by the addition of 10 μL of UDPGA, NCHN was incubated with UGT1A1 (0.06 mg/mL) for 50 min or HLMs (0.2 mg/mL) for 40 min in the presence or absence of different concentrations of icotinib and erlotinib. Then, the reactions was quenched by adding 200 μL of acetonitrile, the incubation mixtures were then centrifuged under the condition of 20,000 × *g*, 4 °C for 20 min to obtain the supernatant. Lastly, 200 μL aliquots of the supernatants were diverted into the 96-well plates, the fluorescence intensity of NCHNG were read by Synergy H1 Hybrid Multi-Mode Microplate Reader (BioTek, USA), under the excitation wavelength of 362 nm and the emission wavelength of 450 nm at a gain setting of 80. The positive control (positive inhibitor, nilotinib) was also carried out under the same conditions. The tested chemicals and inhibitors were all dissolved in dimethyl sulfoxide (DMSO), and the final concentration of DMSO in the incubation system was 1% (*v*/*v*), which has only a minor effect on the catalytic activities of most human UGT enzymes[16]. The concentrations of erlotinib and icotinib presented in the incubations were corrected for binding to HLMs according to the method of equilibrium dialysis[17].

2.3. *Inhibition kinetics analyses*

Inhibition kinetic analysis was performed in both HLMs and recombinant human UGT1A1. IC_{50} values were determined using the same substrate concentration in the presence of different inhibitor concentrations[18–20]. K_i values and the inhibition kinetic types (competitive inhibition, noncompetitive inhibition, uncompetitive inhibition and mixed inhibition) were determined by using various concentrations of NCHN and multiple concentrations of icotinib or erlotinib. IC_{50} values and K_i values were all estimated by the nonlinear regression analysis of Graphpad Prism 6.0 (San Diego, CA, USA). The following equations for competitive inhibition Eq. (1), noncompetitive inhibition Eq. (2), or mixed inhibition Eq. (3) were used to calculate the K_i values[21–23].

$$v = (V_{max}S)/(K_m(1 + I/K_i) + S) \quad (1)$$

$$v = (V_{max}S)/(K_m + S)/(1 + I/K_i) \quad (2)$$

$$v = (V_{max}S)/(K_m + S)(1 + I/\alpha K_i) \quad (3)$$

where v is the velocity of the reaction; K_i is the inhibition constant describing the affinity of the inhibitor for the enzyme; S and I are the substrate and inhibitor concentrations, respectively; V_{max} is the maximum velocity; K_m is the Michaelis constant (substrate concentration at 0.5 V_{max}). Goodness-of-fit parameters were employed to identify the most appropriate inhibition kinetic types.

2.4. *Prediction of the DDI potential in vivo*

The magnitudes of inhibitory interactions mediated by icotinib and erlotinib were estimated by the ratio of AUC in the presence and absence of the inhibitor. This ratio was predicted by using the formula Eq. (4)[24]:

$$\text{AUC ratio} = \frac{1}{f_{hep}\left(\frac{1/E_h}{(1/E_h-1)(1+I/K_i)+1}\right) + (1-f_{hep})} \quad (4)$$

where f_{hep} is the percentage of hepatic clearance mediated by UGT1A1; E_h is the hepatic extraction ratio; K_i (μmol/L) is the inhibitory constant. I is the inhibitor concentration. Taking into account that the free concentration of each inhibitor should be used to predict the inhibitory potentials of erlotinib or icotinib *in vivo*, the binding ratio of erlotinib or icotinib to both human plasma and HLMs were determined. After that, the unbound K_i ($K_{i,u}$) and unbound C_{max} values ($C_{max,u}$), were used for the prediction. In addition, f_{hep} was set at 1 and a wide range of E_h (0.1–0.9) was used to calculate the AUC ratio, due to no f_{hep} and E_h of NCHN were available.

3. Results

3.1. *Inhibition of UGT1A1 activities by icotinib and erlotinib*

The inhibitory effects of icotinib and erlotinib (structures are shown in Fig. 1) against human UGT1A1 were investigated in both recombinant UGT1A1 and HLMs by using NCHN as the specific fluorescent probe substrate for UGT1A1. Firstly, three different concentrations (1, 10 and 100 μmol/L) of icotinib and erlotinib were used to explore their inhibition potentials. As shown in Supplementary information Fig. S1, upon addition of icotinib (10 μmol/L) and erlotinib (10 μmol/L), the residual activities of UGT1A1 were 36% and 19% of the control, respectively. This result suggested that erlotinib displayed relative strong inhibitory effects against UGT1A1-mediated NCHN-4-*O*-glucuronidation. To further investigate the inhibitory potentials of icotinib and erlotinib, the dose-dependent inhibition curves of two compounds against UGT1A1 enzyme were depicted in both recombinant human UGT1A1 and pooled HLMs. As shown in Fig. 2, both compounds could inhibit NCHN-4-*O*-glucuronidation in a dose-dependent manner. As shown in Table 1, the IC_{50} values of icotinib and erlotinib in recombinant human UGT1A1 were evaluated as 8.76 and 0.69 μmol/L, respectively. Meanwhile, the IC_{50} values of icotinib and erlotinib against UGT1A1-mediated NCHN-4-*O*-glucuronidation in HLMs were evaluated as 5.15 and 0.68 μmol/L, respectively. These results clearly demonstrated that both icotinib and erlotinib are UGT1A1 inhibitors, and icotinib displayed relatively weak inhibitory effects against UGT1A1. In addition, no phase II metabolites of erlotinib and icotinib was found in these incubations, which were consistent with previous

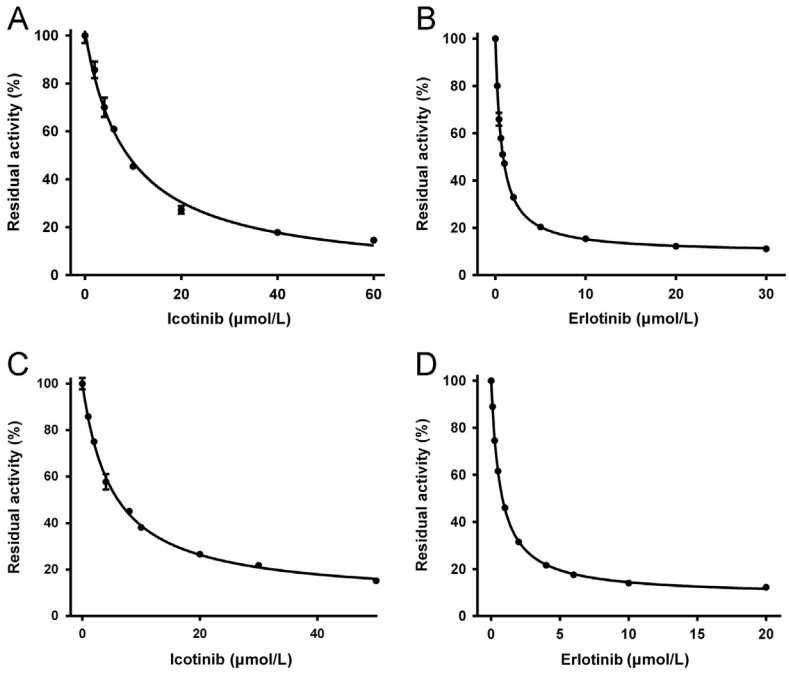

Figure 2 Dose-dependent inhibition curves of icotinib and erlotinib against UGT1A1-mediated NCHN-4-*O*-glucuronidation in recombinant human UGT1A1 (A and B) and HLMs (C and D).

Table 1 Inhibition kinetic parameters of icotinib and erlotinib against UGT1A1-mediated NCHN-4-*O*-glucuronidation in both recombinant human UGT1A1 and HLMs.

Enzyme source	Icotinib			Erlotinib		
	IC_{50} (μmol/L)	K_i (μmol/L)	Inhibition type	IC_{50} (μmol/L)	K_i (μmol/L)	Inhibition type
UGT1A1	8.76 ± 0.78	10.04	Noncompetitive	0.69 ± 0.02	1.72	Noncompetitive
HLM	5.15 ± 0.28	8.55	Noncompetitive	0.68 ± 0.01	1.23	Noncompetitive

reports that CYPs were the major metabolism enzymes for erlotinib and icotinib[25,26]. The inhibition of erlotinib and icotinib against UGT1A1 in HLMs is not time-dependent, implying that erlotinib and icotinib cannot trigger irreversible inhibition against UGT1A1 (data not shown).

3.2. *Inhibition kinetic analyses for icotinib and erlotinib against NCHN-O-glucuronidation in UGT1A1*

Inhibition kinetic assays were further performed to characterize the inhibition types and the inhibition kinetic constants of icotinib and erlotinib against UGT1A1. As shown in Fig. 3 and Supplementary information Fig. S2, both Lineweaver-Burk and Dixon plots demonstrated that icotinib functioned as a noncompetitive inhibitor against NCHN-*O*-glucuronidation in recombinant human UGT1A1. The K_i value of icotinib against NCHN-*O*-glucuronidation in recombinant human UGT1A1 was determined as 10.04 μmol/L (Table 1). In contrast, erlotinib was found to be a more potent noncompetitive inhibitor against UGT1A1. The K_i value of erlotinib against NCHN-*O*-glucuronidation in human UGT1A1 was determined as 1.72 μmol/L (Table 1). These findings demonstrated that both erlotinib and icotinib displayed the same inhibition type (noncompetitive inhibition) against UGT1A1-mediated NCN-4-*O*-glucuronidation, while icotinib exhibited relatively weak inhibitory effect (K_i value of 10.04 μmol/L *versus* 1.72 μmol/L) against UGT1A1 compared to erlotinib.

3.3. *Inhibition kinetic analyses for icotinib and erlotinib against NCHN-O-glucuronidation in HLM*

To further validate whether icotinib and erlotinib could inhibit UGT1A1 in complex biological systems, the inhibition kinetic for icotinib and erlotinib against UGT1A1-mediated NCHN-*O*-glucuronidation were performed in pooled HLMs. As shown in Fig. 4, Table 1 and supplementary information Fig. S2 both Lineweaver-Burk and Dixon plots demonstrated that icotinib and erlotinib displayed noncompetitive inhibition type against UGT1A1-mediated NCHN-*O*-glucuronidation in HLMs, which was in accordance with the inhibition types of icotinib and erlotinib against NCHN-*O*-glucuronidation in recombinant human UGT1A1. The K_i values of icotinib and erlotinib against NCHN-*O*-glucuronidation by UGT1A1 in HLMs were determined as 8.55 and 1.23 μmol/L, respectively. These results demonstrated that erlotinib exhibited more potent inhibitory effects on UGT1A1 in HLMs (about 7-fold for NCHN-*O*-glucuronidation) than that of

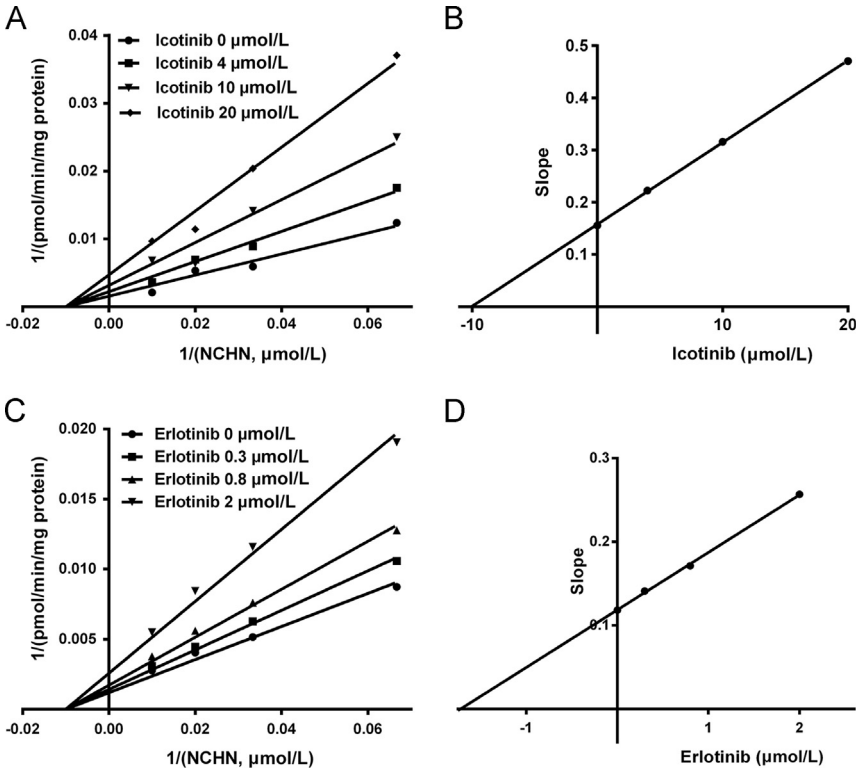

Figure 3 The Lineweaver-Burk plots (A) and the second plot of slopes from Lineweaver-Burk plots (B) for icotinib inhibition on NCHN-*O*-glucuronidation in recombinant human UGT1A1; The Lineweaver-Burk plots (C) and the second plot of slopes from Lineweaver-Burk plots (D) for erlotinib inhibition on NCHN-*O*-glucuronidation in recombinant human UGT1A1.

icotinib, which agreed well with the results obtained from UGT1A1. All these findings demonstrated that both erlotinib and icotinib are noncompetitive inhibitors against UGT1A1-mediated NCHN-*O*-glucuronidation, while icotinib displayed relatively weak inhibition against UGT1A1.

3.4. Quantitative prediction of DDI risks of icotinib and erlotinib

The inhibition potentials of icotinib and erlotinib against human UGT1A1 and the clinical DDI risk *in vivo* were evaluated by estimating the changes in AUC of NCHN predominantly metabolized by UGT1A1. Following oral administration of icotinib (125 mg × 3 daily) and erlotinib (150 mg daily), the maximum plasma concentration of icotinib and erlotinib in human was 4.79 and 6.06 μmol/L, respectively[27,28]. The $C_{max,u}$ of erlotinib and icotinib were calculated as 0.55 and 0.53 μmol/L, respectively. The corrected $K_{i,u}$ and uncorrected K_i values of icotinib and erlotinib against UGT1A1-mediated NCHN-*O*-glucuronidation in HLMs were much closed to each other, due to the negligible binding of icotinib and erlotinib to proteins in HLMs. The predicted AUC ratio and the increased percent were listed in Table 2. The AUC of NCHN would be increased by 5%–43% following administration of erlotinib (150 mg daily), while the AUC of NCHN was slightly increased by 1%–6% following administration of icotinib (125 mg × 3 daily). These results suggested that icotinib was unlikely to cause a significant DDI through inhibition of UGT1A1, while erlotinib exhibited much higher DDI potentials.

4. Discussion

Recently, TKIs have proven to be an effective therapy to treat certain forms of cancers including non-small cell lung cancer, pancreatic cancer, and chronic myeloid leukaemia due to their selective and potent inhibition of tumour cells *in vitro*[29]. Unfortunately, the use of majority of TKIs are reported to be associated with serious toxic effects on a number of vital organs including the liver[11]. Erlotinib is a TKI with a boxed label warning due to hepatotoxicity, thus needs to be carefully monitored for patients, which is recommended by FDA[11]. It is noteworthy that erlotinib has been reported to exhibit strong inhibitory effects on UGT1A1 and may result in potential DDI. As the first home-grown anticancer drug developed by Chinese pharmaceutical company (Zhejiang Beta Pharma, Inc., Zhejiang, China), icotinib is structurally similar with erlotinib, implying that icotinib may act on the same targets as erlotinib. It is well known that erlotinib is a potent inhibitor of UGT1A1, while strong inhibition of UGT1A1 may lead to hepatotoxicity including hyperbilirubinemia, kernicterus and drug-induced liver injury[7,30]. Thus, it is necessary to carefully investigate the inhibitory effects of erlotinib derivatives (such as icotinib) on UGT1A1. However, until now, the inhibitory potency of icotinib on UGT1A1 has not been well investigated, and the differences in UGT1A1 inhibition and potential risk between icotinib and erlotinib have not been clearly evaluated. In these cases, this study focused on the investigation and comparison of the inhibitory effects of icotinib and erlotinib on human UGT1A1 and evaluated their potential DDI risk due to UGT1A1 inhibition.

In this study, the inhibitory effects of icotinib and erlotinib against human UGT1A1 were carefully investigated and compared

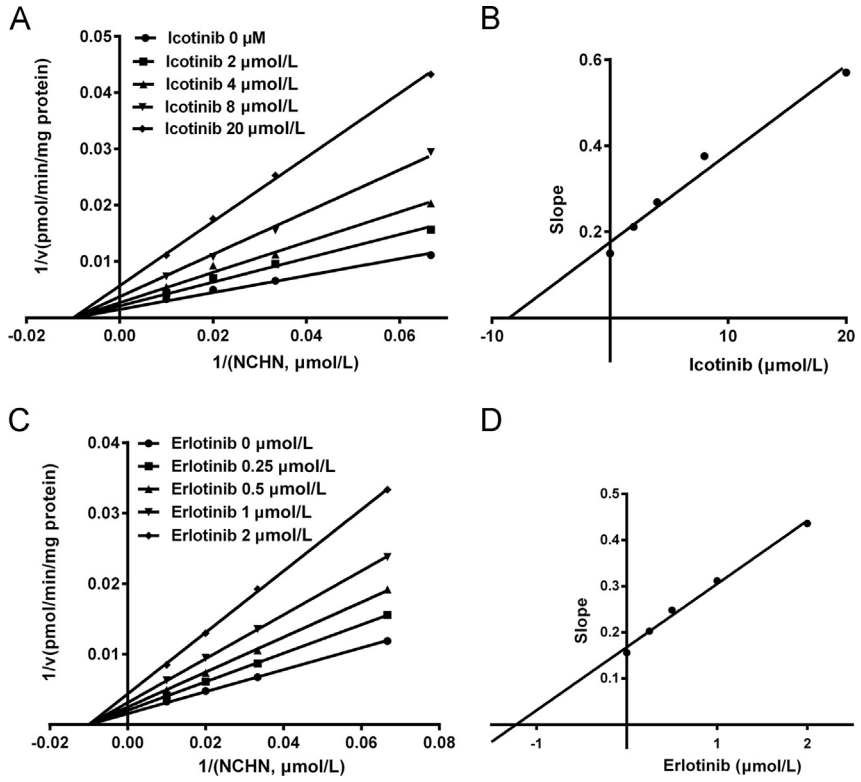

Fig. 4 The Lineweaver-Burk plots (A) and the second plot of slopes from Lineweaver-Burk plots (B) for icotinib inhibition on NCHN-*O*-glucuronidation in HLMs; The Lineweaver-Burk plots (C) and the second plot of slopes from Lineweaver-Burk plots (D) for erlotinib inhibition on NCHN-*O*-glucuronidation in HLMs.

Table 2 Prediction of the potential DDI risks *in vivo* based on the AUC ratios.

Inhibitor	Enzyme source	E_h[a]	f_{hep}[b]	$K_{i,u}$[c] (μmol/L)	$C_{max,u}$[d] (μmol/L)	AUC ratios[e]	AUC increased (%)
Icotinib	HLM	0.1–0.9	1	8.55	0.53	1.01–1.06	1%–6%
Erlotinib	HLM	0.1–0.9	1	1.23	0.55	1.05–1.43	5%–43%

[a]E_h is the hepatic extraction ratio ranging from 0.1 to 0.9 for UGT1A1 substrates.
[b]The f_{hep} was set to 1.
[c]The $K_{i,u}$ values of erlotinib and icotinib is the same to the K_i values, due to the negligible binding of erlotinib or icotinib to HLMs (0.2 mg/mL).
[d]The C_{max} of icotinib in humans was 4.79 μmol/L after a 125 mg × 3 daily dose of icotinib hydrochloride; The C_{max} of erlotinib in humans was 6.06 μmol/L after a single 150 mg dose of erlotinib. The unbound C_{max} of erlotinib or icotinib ($C_{max,u}$) were calculated as $C_{max} \times f_u$ (f_u was determined as 0.09 and 0.11 for erlotinib and icotinib, respectively).
[e]Prediction methods as described in the materials and method.

to each other. The results clearly demonstrated that both icotinib and erlotinib are UGT1A1 inhibitors as we assumed, but icotinib exhibited relatively weak inhibitory effect against UGT1A1 compared to erlotinib. The inhibition potency (IC_{50}) of erlotinib on UGT1A1 in both recombinant UGT1A1 and HLMs is less than 1 μmol/L, which is more potent than that of icotinib in these enzyme sources (>5 μmol/L). Furthermore, inhibition kinetic analysis was performed to characterize and evaluate the inhibition types and inhibition constants of icotinib and erlotinib. The results clearly demonstrated that both compounds functioned as non-competitive inhibitors against NCHN-*O*-glucuronidation in both recombinant human UGT1A1 and HLMs, while the K_i values of icotinib is relatively greater than that of erlotinib. All these findings suggested that erlotinib is a potent inhibitor against UGT1A1, but icotinib is a moderate inhibitor against UGT1A1.

From the view of chemical structure, both icotinib and erlotinib have a same quinazoline skeleton, but the side-chain of icotinib has a feature of closed ring structure, which makes it to be more hydrophobic[31,32]. The similar structure makes icotinib and erlotinib act on the same biological targets including EGFR and UGT1A1, but the subtle difference in chemical structure may change the potency of these two agents towards the same target. In this study, we compare the inhibitory potency of icotinib and erlotinib against UGT1A1, our results shown that both compounds display the same inhibition types against UGT1A1, but the subtle difference in chemical structure between them leads to the alteration in inhibitory effects of these two agents on UGT1A1. In contrast to erlotinib, icotinib displayed relatively low affinity towards UGT1A1, the K_i value of icotinib (8.55 μmol/L in HLMs) is about 7-fold than that of erlotinib (1.23 μmol/L in HLMs). All

these findings suggested that the subtle change in the side-chains of erlotinib to a closed ring chain can decrease the inhibition on UGT1A1, which could be used to partially explain why icotinib displayed improved safety profile (such as very low incidence of liver function impairment) in contrast to erlotinib.

With the inhibition constant (K_i) of these two TKIs in hands, the magnitudes of the potential inhibitory effects of them on UGT1A1 *in vivo* were also predicted by estimating the changes in AUC ratios. Based on the $C_{max,u}$ and $K_{i,u}$ values, the AUC of NCHN would be increased by 5%–43% following administration of erlotinib (150 mg daily), while the AUC of NCHN was slightly increased by 1%–6% following administration of icotinib (125 mg × 3 daily). Thus, the results suggested that erlotinib exhibited much higher DDI potentials than icotinib *via* UGT1A1 inhibition, which was consistent with the clinical observation that icotinib displayed improved safety profile (such as very low incidence of liver function impairment) in contrast to erlotinib. It should be noted that the inhibitory effects of icotinib or erlotinib on UGT1A1 should be taken with caution in some special populations. It is well-known that UGT1A1 is a highly polymorphic enzyme, and more than one hundred variants have been found[33]. Some polymorphic expression of certain UGT1A1 mutants may result in partial or complete loss of UGT1A1 activity, the exposure of icotinib and erlotinib to these individuals may bring strong effects on UGT1A1-mediated metabolism[34]. Thus, the individuals with UGT1A1 variants that possessing low catalytic activity might be expected to manifest heightened susceptibility to serious toxic effects as a consequence of inhibition of UGT1A1 by icotinib and erlotinib. Furthermore, erlotinib could be metabolized in human primarily by CYP3A4, CYP3A5, CYP1A1 and CYP1A2, while the primarily enzymes for icotinib was CYP3A4 and CYP2C19[25,26]. Several genetic polymorphisms within these CYPs gene, especially in subjects carrying activity decreasing alleles, might cause high systemic exposure of erlotinib or icotinib. As a result, the concentrations of icotinib or erlotinib in the blood may exceed the maximum concentrations used here in predicting the AUC ratio and thus bring undesirable effects[35]. In these cases, the potential risks of icotinib or erlotinib *via* UGT1A1 inhibition should be fully considered.

In summary, our results demonstrated that icotinib and erlotinib displayed inhibitory effects on human UGT1A1, while icotinib exhibited relatively weak inhibition against UGT1A1 catalytic activity in HLM compared to erlotinib. In addition, icotinib was unlikely to cause a significant DDI through inhibition of UGT1A1, while erlotinib exhibited much higher DDI potentials. Our findings shed light on the underlying mechanisms of clinically significant hepatotoxicity associated with erlotinib and partially account for the differential hepatic toxicity observed between icotinib and erlotinib. All these findings reveal that the subtle differences in chemical structure between icotinib and erlotinib bring different inhibition potency on UGT1A1, which are very helpful for the medicinal chemists to design and develop next generation TKIs with improved safety. Meanwhile, these findings are very useful for guiding reasonable applications of icotinib and erlotinib in clinic, especially for avoiding the potential DDI risks caused by them *via* UGT1A1 inhibition.

Acknowledgments

This project was financially supported by National Natural Science Foundation of China (81403002, 81473181, and 81573501), the First Affiliated Hospital of Zhengzhou University (201613) and Innovative Entrepreneurship Program of High-Level Talents in Dalian (2016RQ025).

Appendix A. Supplementary material

Supplementary data associated with this article can be found in the online version at http://dx.doi.org/10.1016/j.apsb.2017.07.004.

References

1 Wang XX, Lv X, Li SY, Hou J, Ning J, Wang JY, et al. Identification and characterization of naturally occurring inhibitors against UDP-glucuronosyltransferase 1A1 in Fructus Psoraleae (Bu-gu-zhi). *Toxicol Appl Pharmacol* 2015;**289**:70–8.
2 Brierley CH, Burchell B. Human UDP-glucuronosyl transferases: chemical defence, jaundice and gene therapy. *Bioessays* 1993;**15**:749–54.
3 Ma G, Wu B, Gao S, Yang Z, Ma Y, Hu M. Mutual regioselective inhibition of human UGT1A1-mediated glucuronidation of four flavonoids. *Mol Pharm* 2013;**10**:2891–903.
4 Lv X, Ge GB, Feng L, Troberg J, Hu LH, Hou J, et al. An optimized ratiometric fluorescent probe for sensing human UDP-glucuronosyltransferase 1A1 and its biological applications. *Biosens Bioelectron* 2015;**72**:261–7.
5 Liu Y, Ramirez J, House L, Ratain MJ. Comparison of the drug–drug interactions potential of erlotinib and gefitinib via inhibition of UDP-glucuronosyltransferases. *Drug Metab Dispos* 2010;**38**:32–9.
6 Miners JO, Chau N, Rowland A, Burns K, McKinnon RA, Mackenzie PI, et al. Inhibition of human UDP-glucuronosyltransferase enzymes by lapatinib, pazopanib, regorafenib and sorafenib: implications for hyperbilirubinemia. *Biochem Pharmacol* 2017;**129**:85–95.
7 Ai L, Zhu LL, Yang L, Ge GB, Cao YF, Liu Y, et al. Selectivity for inhibition of nilotinib on the catalytic activity of human UDP-glucuronosyltransferases. *Xenobiotica* 2014;**44**:320–5.
8 Ranieri G, Pantaleo M, Piccinno M, Roncetti M, Mutinati M, Marech I, et al. Tyrosine kinase inhibitors (TKIs) in human and pet tumours with special reference to breast cancer: a comparative review. *Crit Rev Oncol Hematol* 2013;**88**:293–308.
9 Giordani E, Zoratto F, Strudel M, Papa A, Rossi L, Minozzi M, et al. Old tyrosine kinase inhibitors and newcomers in gastrointestinal cancer treatment. *Curr Cancer Drug Targets* 2016;**16**:175–85.
10 Hartmann JT, Haap M, Kopp HG, Lipp HP. Tyrosine kinase inhibitors —a review on pharmacology, metabolism and side effects. *Curr Drug Metab* 2009;**10**:470–81.
11 Shah RR, Morganroth J, Shah DR. Hepatotoxicity of tyrosine kinase inhibitors: clinical and regulatory perspectives. *Drug Saf* 2013;**36**:491–503.
12 Rong BX, Liu H, Gao WL, Ying SY. Efficacy and safety of icotinib in treating non-small cell lung cancer: a systematic evaluation and meta-analysis based on 15 studies. *Oncotarget* 2016;**7**:86902–13.
13 Li X, Qin N, Wang J, Yang X, Zhang X, Lv J, et al. Clinical observation of icotinib hydrochloride for advanced non-small cell lung cancer patients with EGFR status identified. *Chin J Lung Cancer* 2015;**18**:734–9.
14 Pan H, Liu R, Li S, Fang H, Wang Z, Huang S, et al. Effects of icotinib on advanced non-small cell lung cancer with different EGFR phenotypes. *Cell Biochem Biophys* 2014;**70**:553–8.
15 Fang ZZ, Cao YF, Hu CM, Hong M, Sun X, Ge GB, et al. Structure-inhibition relationship of ginsenosides towards UDP-glucuronosyltransferases (UGTs). *Toxicol Appl Pharmacol* 2013;**267**:149–54.
16 Uchaipichat V, Mackenzie PI, Guo XH, Gardner-Stephen D, Galetin A, Houston JB, et al. Human UDP-glucuronosyltransferases: isoform selectivity and kinetics of 4-methylumbelliferone and 1-naphthol glucuronidation, effects of organic solvents, and inhibition by diclofenac and probenecid. *Drug Metab Dispos* 2004;**32**:413–23.

17 Burns K, Nair PC, Rowland A, Mackenzie PI, Knights KM, Miners JO. The nonspecific binding of tyrosine kinase inhibitors to human liver microsomes. *Drug Metab Dispos* 2015;**43**:1934–7.
18 Lei W, Wang DD, Dou TY, Hou J, Feng L, Yin H, et al. Assessment of the inhibitory effects of pyrethroids against human carboxylesterases. *Toxicol Appl Pharmacol* 2017;**321**:48–56.
19 He W, Wu JJ, Ning J, Hou J, Xin H, He YQ, et al. Inhibition of human cytochrome P450 enzymes by licochalcone A, a naturally occurring constituent of licorice. *Toxicol Vitr* 2015;**29**:1569–76.
20 Li YG, Hou J, Li SY, Lv X, Ning J, Wang P, et al. Fructus Psoraleae contains natural compounds with potent inhibitory effects towards human carboxylesterase 2. *Fitoterapia* 2015;**101**:99–106.
21 Zhu L, Xiao L, Xia Y, Zhou K, Wang H, Huang M, et al. Diethylstilbestrol can effectively accelerate estradiol-17-*O*-glucuronidation, while potently inhibiting estradiol-3-*O*-glucuronidation. *Toxicol Appl Pharmacol* 2015;**283**:109–16.
22 Xin H, Qi XY, Wu JJ, Wang XX, Li Y, Hong JY, et al. Assessment of the inhibition potential of licochalcone A against human UDP-glucuronosyltransferases. *Food Chem Toxicol* 2016;**90**:112–22.
23 Weng ZM, Wang P, Ge GB, Dai ZR, Wu DC, Zou LW, et al. Structure–activity relationships of flavonoids as natural inhibitors against *E. coli* β-glucuronidase. *Food Chem Toxicol* 2017.
24 Kirby BJ, Unadkat JD. Impact of ignoring extraction ratio when predicting drug–drug interactions, fraction metabolized, and intestinal first-pass contribution. *Drug Metab Dispos* 2010;**38**:1926–33.
25 Ni J, Zhang L. Evaluation of three small molecular drugs for targeted therapy to treat nonsmall cell lung cancer. *Chin Med J (Engl)* 2016;**129**:332–40.
26 Chen J, Liu D, Zheng X, Zhao Q, Jiang J, Hu P. Relative contributions of the major human CYP450 to the metabolism of icotinib and its implication in prediction of drug–drug interaction between icotinib and CYP3A4 inhibitors/inducers using physiologically based pharmacokinetic modeling. *Expert Opin Drug Metab Toxicol* 2015;**11**:857–68.
27 Ni J, Liu DY, Hu B, Li C, Jiang J, Wang HP, et al. Relationship between icotinib hydrochloride exposure and clinical outcome in Chinese patients with advanced non-small cell lung cancer. *Cancer* 2015;**121**(17)3146–56.
28 Yamamoto N, Horiike A, Fujisaka Y, Murakami H, Shimoyama T, Yamada Y, et al. Phase I dose—finding and pharmacokinetic study of the oral epidermal growth factor receptor tyrosine kinase inhibitor Ro50-8231 (erlotinib) in Japanese patients with solid tumors. *Cancer Chemother Pharmacol* 2008;**61**:489–96.
29 Liu DY, Jiang J, Zhang L, Tan FL, Wang YX, Zhang D, et al. Clinical pharmacokinetics of icotinib, an anti-cancer drug: evaluation of dose proportionality, food effect, and tolerability in healthy subjects. *Cancer Chemother Pharmacol* 2014;**73**:721–7.
30 Lv X, Wang XX, Hou J, Fang ZZ, Wu JJ, Cao YF, et al. Comparison of the inhibitory effects of tolcapone and entacapone against human UDP-glucuronosyltransferases. *Toxicol Appl Pharmacol* 2016;**301**:42–9.
31 Tan F, Shi Y, Wang Y, Ding L, Yuan X, Sun Y. Icotinib, a selective EGF receptor tyrosine kinase inhibitor, for the treatment of non-small-cell lung cancer. *Future Oncol* 2015;**11**:385–97.
32 Cascone T, Morelli MP, Ciardiello F. Small molecule epidermal growth factor receptor (EGFR) tyrosine kinase inhibitors in non-small cell lung cancer. *Ann Oncol* 2006;**17**:46–8.
33 Court MH. Interindividual variability in hepatic drug glucuronidation: studies into the role of age, sex, enzyme inducers, and genetic polymorphism using the human liver bank as a model system. *Drug Metab Rev* 2010;**42**:209–24.
34 Guillemette C, Levesque E, Rouleau M. Pharmacogenomics of human uridine diphospho-glucuronosyltransferases and clinical implications. *Clin Pharmacol Ther* 2014;**96**:324–39.
35 Miners JO, Knights KM, Houston JB, Mackenzie PI. *In vitro–in vivo* correlation for drugs and other compounds eliminated by glucuronidation in humans: pitfalls and promises. *Biochem Pharmacol* 2006;**71**:1531–9.